Electronic Supplementary Material (ESI) for Journal of Materials Chemistry C.

Supporting Information

High-efficiency organic electroluminescent materials based on D-A-D type with sterically hindered methyl groups

Youming Zhang,[ab] Xuan Zhou,[ad] Changjiang Zhou,[b] Qiang Su,[c] Shuming Chen,[c]* Jun Song[d] and Wai-Yeung Wong[a]*

[a] *Department of Applied Biology and Chemical Technology, The Hong Kong Polytechnic University, Hung Hom, Hong Kong, P. R. China*

[b] *College of Materials Science and Engineering, Shenzhen University, Shenzhen 518060, China*

[c] *Department of Electrical and Electronic Engineering, Southern University of Science and Technology, Shenzhen, 518055, P. R. China*

[d] *Key Laboratory of Optoelectronic Devices and Systems of Ministry of Education and Guangdong Province, College of Physics and Optoelectronic Engineering, Shenzhen University, Shenzhen 518060, P. R. China*

E-mail: wai-yeung.wong@polyu.edu.hk; chen.sm@sustc.edu.cn

1. General considerations for characterization

Instrument: Nuclear magnetic resonance (NMR) spectra were recorded on a Bruker DRX 400 spectrometer using tetramethylsilane as a reference in deuterated chloroform solution at 298 K. MALDI-TOF mass spectrometric measurements were

performed on a Bruker Bifiex III MALDI-TOF spectrometer. Thermogravimetric analysis (TGA) was conducted under a dry nitrogen gas flow at a heating rate of 10 ^{o}C min^{-1} on a Perkin- Elmer TGA 7. UV-Vis absorption spectra were recorded on a HP-8453 UV-visible system. Cyclic voltammetry was carried out on a CHI660A electrochemical work station in a three-electrode cell dipped in a 0.1 M tetrabutylammonium hexafluorophosphate (Bu_4NPF_6) acetonitrile solution under nitrogen protection at a scan rate of 100 mV s^{-1} and room temperature (RT). In this three-electrode cell, a platinum rod, platinum wire and Ag/AgCl electrode were used as a working electrode, counter electrode and reference electrode, respectively. Ferrocene was added as the internal standard. Steady state fluorescence spectra, fluorescence lifetime, and quantum efficiency were measured with Edinburgh fluorescence spectrometer (FLS980) with an integrating sphere. Lifetime in the time range from 0 ns to 150 ns was measured using picosecond pulsed diode laser under the excitation at 375 nm. The DFT calculations were performed with the Gaussian09 series of programs using the B3LYP hybrid functional and 6-31G(d, p) basis set.

2. Device fabrication and characterization

The layers of ITO/HATCN (20 nm)/TAPC (40 nm)/emitter:*m*CP (5 wt%, 15 nm)/TmPyPB (50 nm)/LiF (1 nm)/Al (100 nm) were successively deposited on the pre-cleaned ITO glass substrates at a pressure of less than 10^{-4} Torr. The active area of devices was 2 mm × 2 mm. The EL spectra of devices were measured by fiber optic spectrometer (Ocean Optics USB 2000) in the normal direction. The *J-V-L* curves

were investigated by a dual-channel Keithley 2614B source measure unit and a PIN-25D silicon photodiode. All the measurements were conducted at room temperature under ambient condition.

3. Computational details

The molecular geometries, the energy levels of frontal molecular orbitals, frequencies and excitations of molecules were calculated using density functional theory (DFT) at B3LYP/6-31G(d) basis set using Gaussian 09 Rev D.01. For simplicity of calculations, methyl group was used as the side-chain substituent.[2] The molecular orbital distributions were plotted with iso-value of 0.02 and 30 excited states were assumed to calculate the computational spectra of molecules using time-dependent (TD)-DFT at the same level. In order to examine the character of excited-states, natural transition orbitals (NTOs) were evaluated for the five lowest excited-states, involving both singlet and triplet states. This approach provides the most compact representation of the electronic transitions in terms of an expansion into single particle orbitals by diagonalizing the transition density matrix associated with each excitation.

4. Lippert-Mataga calculation

The influence of solvent environment on the optical property of our compounds can be understood using the Lippert-Mataga equation, a model that describes the interactions between the solvent and the dipole moment of solute:

$$hc(v_a - v_f) = hc(v_a^0 - v_f^0) + \frac{2(\mu_e - \mu_g)^2}{a^3} f(\varepsilon,n) \qquad 1\text{-}1$$

where f is the orientational polarizability of the solvent, $\nu_a^0 - \nu_f^0$ corresponds to the Stokes shifts when f is zero, μ_e is the excited state dipole moment, μ_g is the ground-state dipole moment (can be calculated by TDDFT); a is the solvent cavity (Onsager) radius, derived from the Avogadro number (N), molecular weight (M), and density (d = 1.0 g/cm^3); ε and n are the solvent dielectric and the solvent refractive index, respectively; $f(\varepsilon, n)$ and a can be calculated respectively as follows:

$$f(\varepsilon,n) = \frac{\varepsilon - 1}{2\varepsilon + 1} - \frac{n^2 - 1}{2n^2 + 1}$$

1-2

$$a = \left(\frac{3M}{4N\pi d}\right)^{1/3}$$

1-3

According to 1-1, 1-2 and1-3, the μ_e can be calculated as follows:

$$\mu_e = \mu_g + \left\{\frac{hca^3}{2} \times \left[\frac{d(\nu_a - \nu_f)}{df(\varepsilon,n)}\right]\right\}_{1/2}$$

1-4

Equation 1-4 shows that μ_e is proportional to $\left(\frac{d(\nu_a - \nu_f)}{df(\varepsilon,n)}\right)_{1/2}$.

Table 1. Crystal data and structure refinement for 2TPA-BT, 2MeTPA-BT and 2DMeTPA-BT

Identification code	**2TPA-BT**	**2MeTPA-BT**	**2DMeTPA-BT**
Empirical formula	$C_{58}H_{62}N_4S$	$C_{60}H_{66}N_4S$	$C_{62}H_{70}N_4S$
Formula weight	847.17	875.22	903.28
Temperature/K	100.00(10)	100.01(10)	100.00(10)
Crystal system	triclinic	triclinic	monoclinic
Space group	*P*-1	*P*-1	$P2_1/n$
a/Å	10.5957(9)	10.6469(4)	12.4016(3)
b/Å	11.7812(10)	13.3025(5)	24.5755(7)
c/Å	20.1419(12)	18.9893(7)	18.4934(4)
α/°	78.686(6)	107.170(3)	90
β/°	86.684(6)	93.133(3)	95.000(2)
γ/°	77.498(7)	90.910(3)	90
Volume/Å^3	2406.7(3)	2564.31(17)	5614.9(2)
Z	2	2	4
ρ_{calc}g/cm^3	1.169	1.134	1.069
μ/mm^{-1}	0.907	0.866	0.804
F(000)	908.0	940.0	1944.0
Crystal size/mm^3	0.12 × 0.11 × 0.09	0.13 × 0.12 × 0.11	0.13 × 0.11 × 0.1
Radiation	CuKα (λ = 1.54184)	CuKα (λ = 1.54184)	CuKα (λ = 1.54184)
2Θ range for data collection/°	4.474 to 147.19	4.88 to 147.886	5.996 to 147.1
Index ranges	$-11 \le h \le 12$, $-14 \le k \le 14$, $-25 \le l \le 22$	$-13 \le h \le 8$, $-16 \le k \le 16$, $-20 \le l \le 23$	$-15 \le h \le 10$, $-26 \le k \le 30$, $-21 \le l \le 22$

Reflections collected	16600	17404	23309
Independent reflections	9394 [R_{int} = 0.1195, R_{sigma} = 0.1394]	10025 [R_{int} = 0.0459, R_{sigma} = 0.0546]	11010 [R_{int} = 0.0525, R_{sigma} = 0.0653]
Data/restraints/parameters	9394/0/580	10025/0/600	11010/0/620
Goodness-of-fit on F^2	1.054	1.054	1.030
Final R indexes [I≥2σ (I)]	R_1 = 0.0894, wR_2 = 0.2064	R_1 = 0.0746, wR_2 = 0.2081	R_1 = 0.0730, wR_2 = 0.2004
Final R indexes [all data]	R_1 = 0.1100, wR_2 = 0.2447	R_1 = 0.0860, wR_2 = 0.2246	R_1 = 0.0943, wR_2 = 0.2215
Largest diff. peak/hole / e $Å^{-3}$	0.71/-0.43	0.56/-0.71	0.83/-0.43

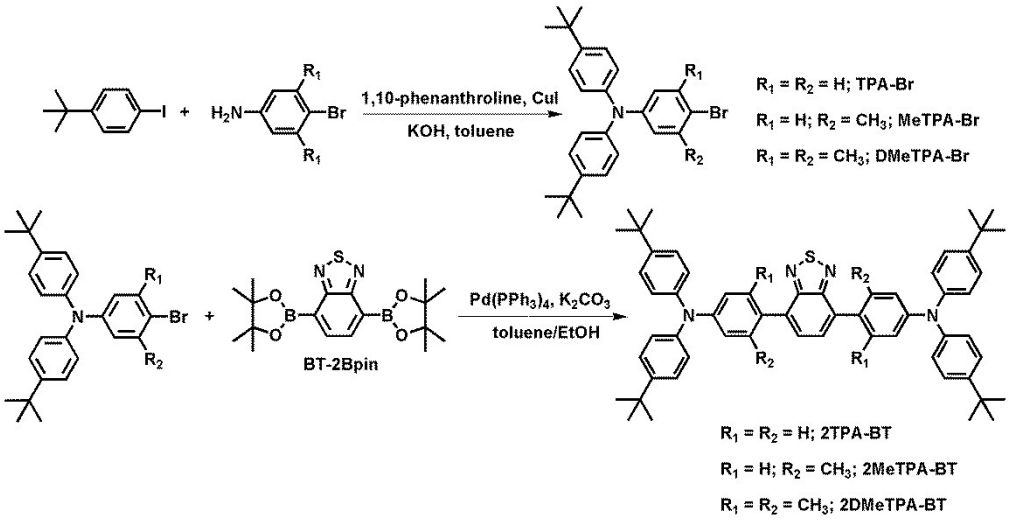

Figure S1. Synthetic routes of **2TPA-BT**, **2MeTPA-BT** and **2DMeTPA-BT**

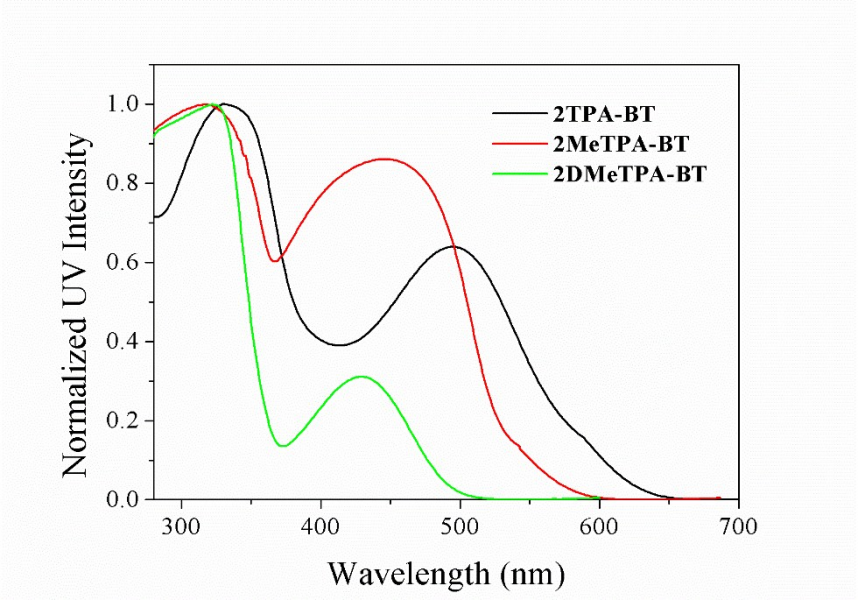

Figure S2. UV–vis absorption spectra of **2TPA-BT**, **2MeTPA-BT** and **2DMeTPA-BT** in neat films

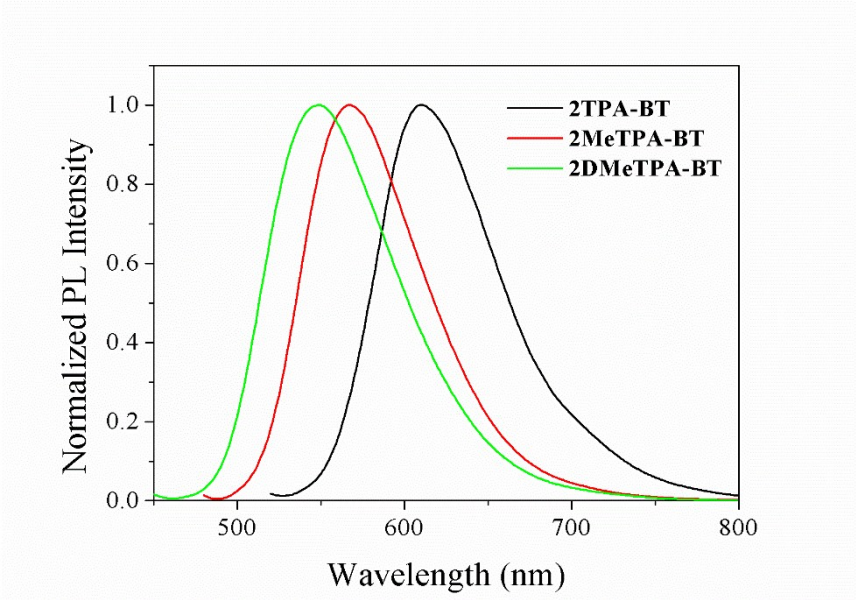

Figure S3. PL spectra of **2TPA-BT**, **2MeTPA-BT** and **2DMeTPA-BT** in neat films

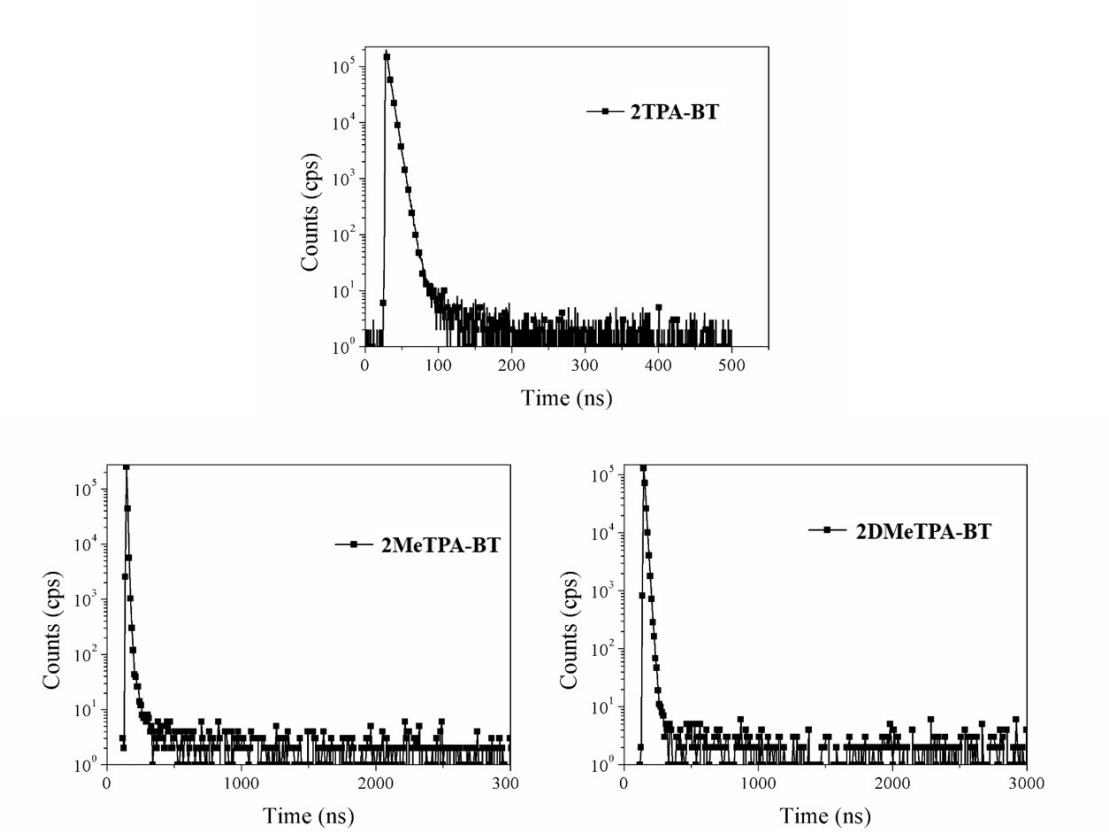

Figure S4. Lifetime measurements of **2TPA-BT**, **2MeTPA-BT** and **2DMeTPA-BT** in neat films

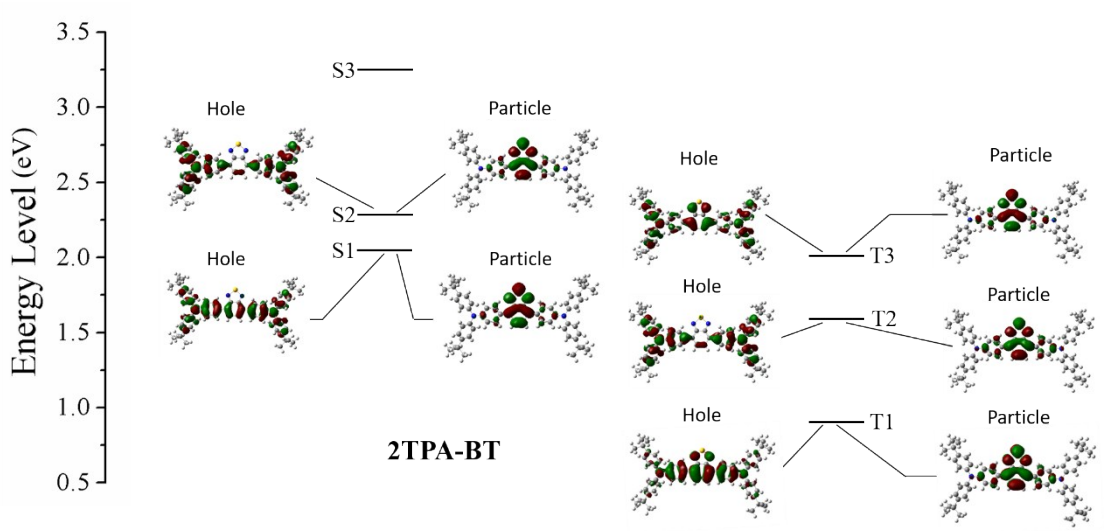

Figure S5. The energy level and the natural transition orbitals of S_1, S_2, T_1, T_2 and T_3 for **2TPA-BT**.

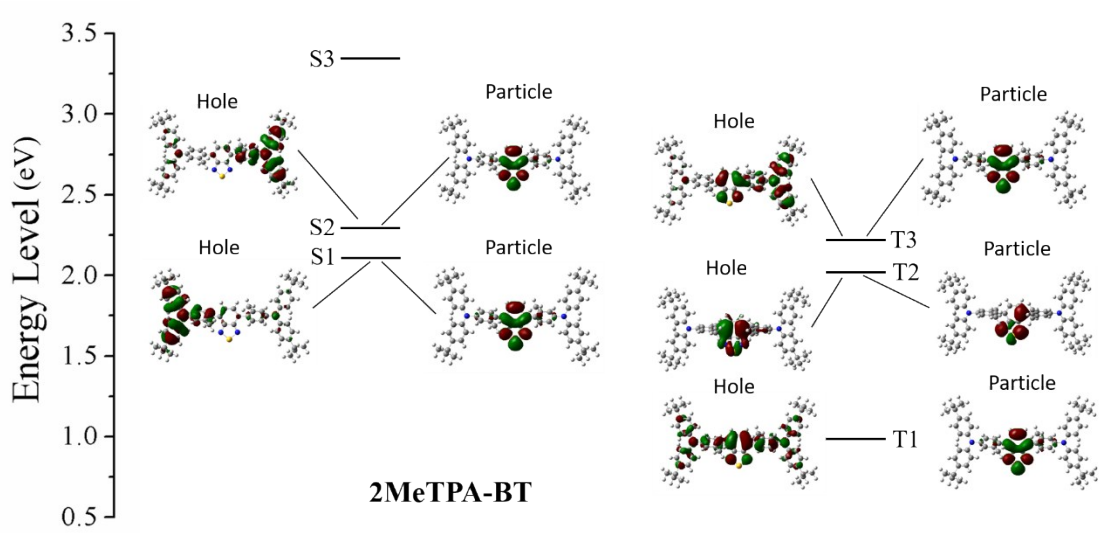

Figure S6. The energy level and the natural transition orbitals of S_1, S_2, T_1, T_2 and T_3 for **2MeTPA-BT**.

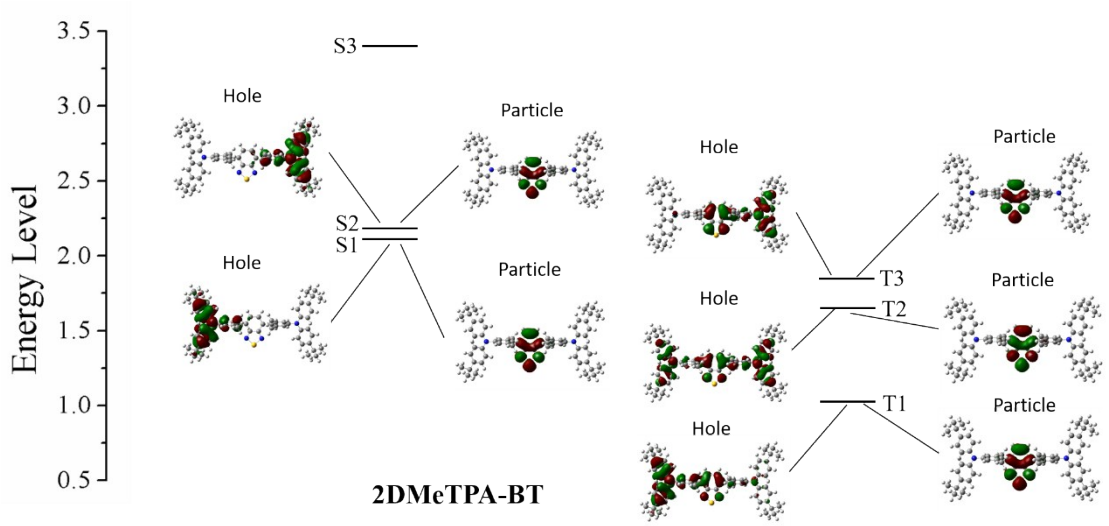

Figure S7. The energy level and the natural transition orbitals of S_1, S_2, T_1, T_2, T_3 and T_5 for **2DMeTPA-BT**.

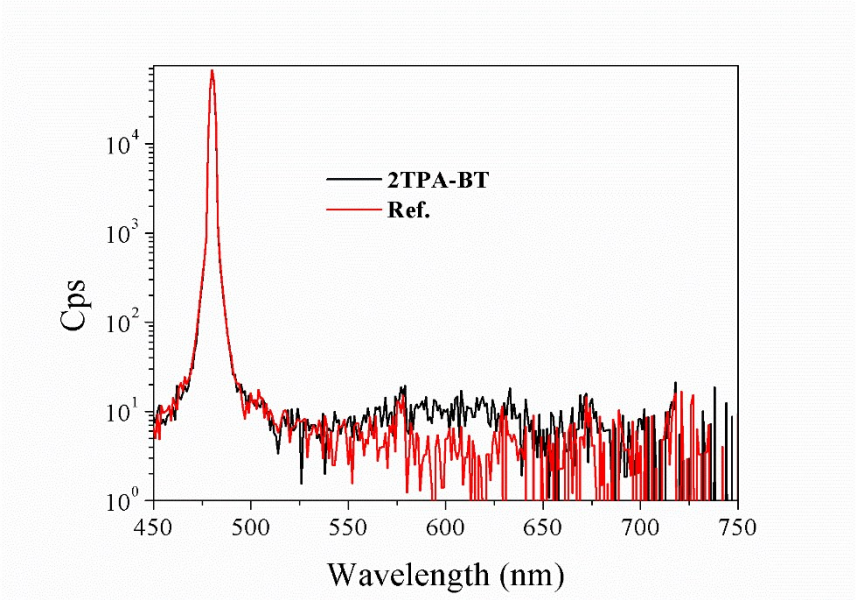

Figure S8. Emission spectra of xenon lamp and **2TPA-BT**:*m*CP composed film.

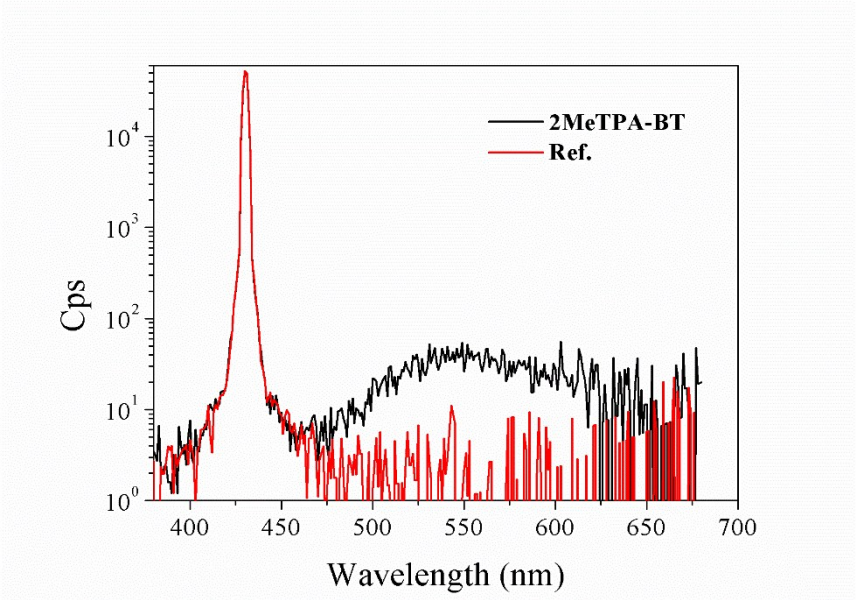

Figure S9. Emission spectra of xenon lamp and **2MeTPA-BT**:*m*CP composed film.

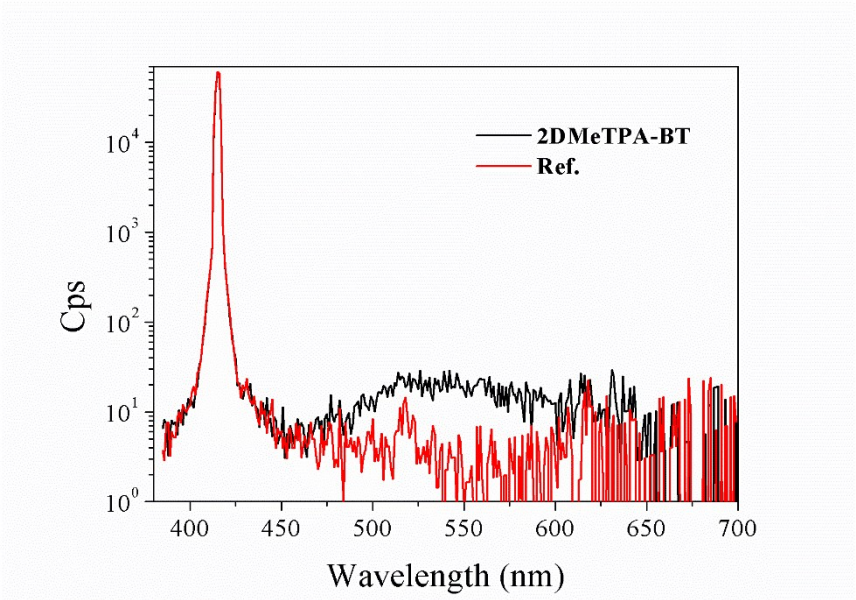

Figure S10. Emission spectra of xenon lamp and **2DMeTPA-BT**:*m*CP composed film.

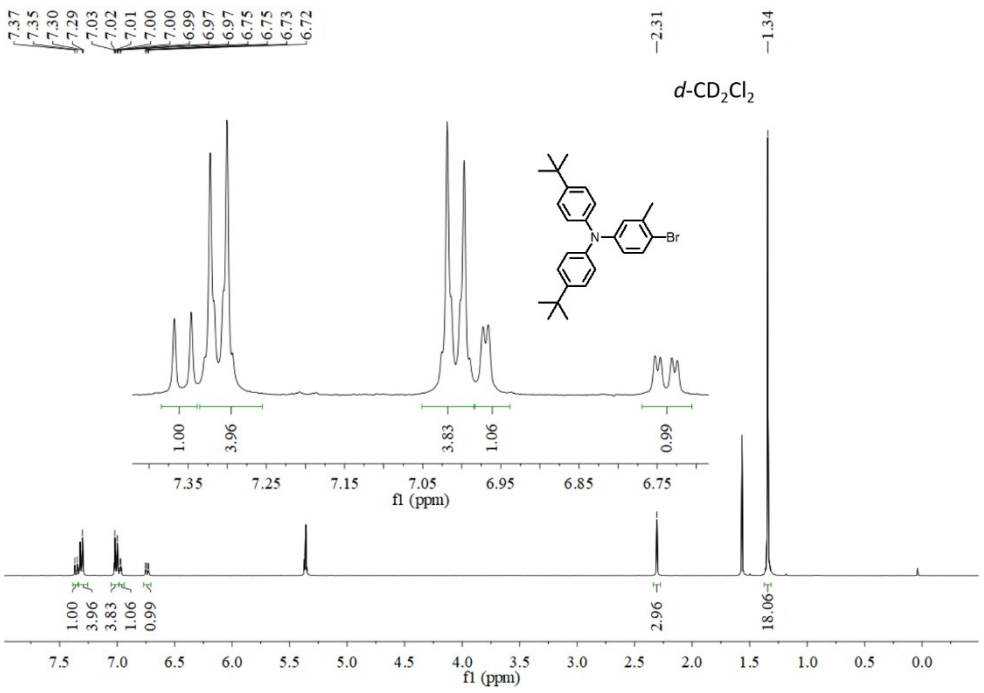

Figure S11. [1]H NMR spectrum of **MeTPA-Br**

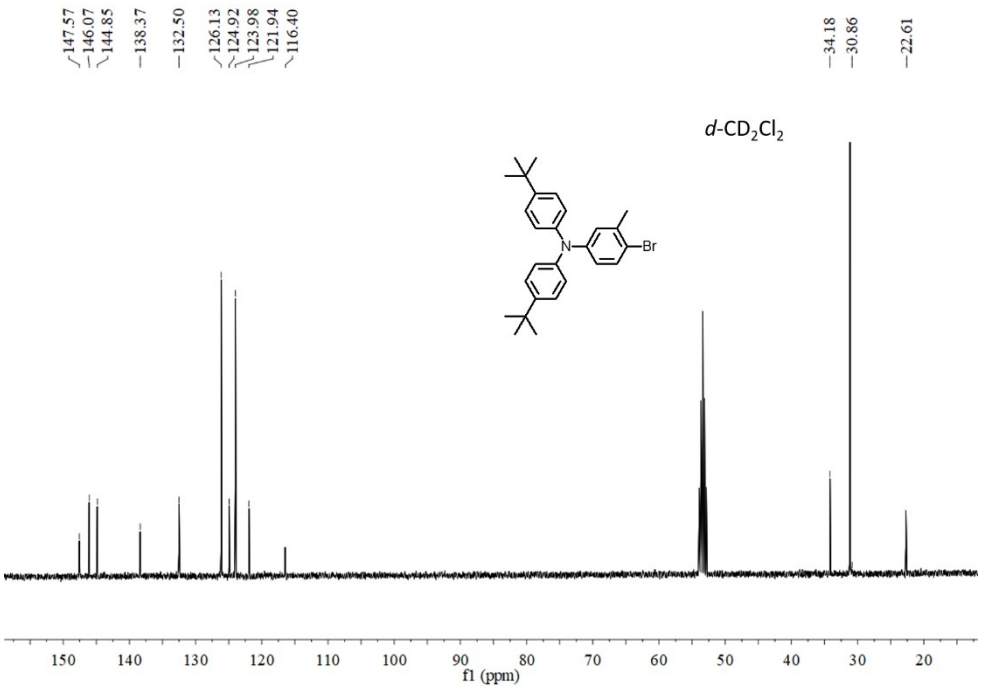

Figure S12. [13]C NMR spectrum of **MeTPA-Br**

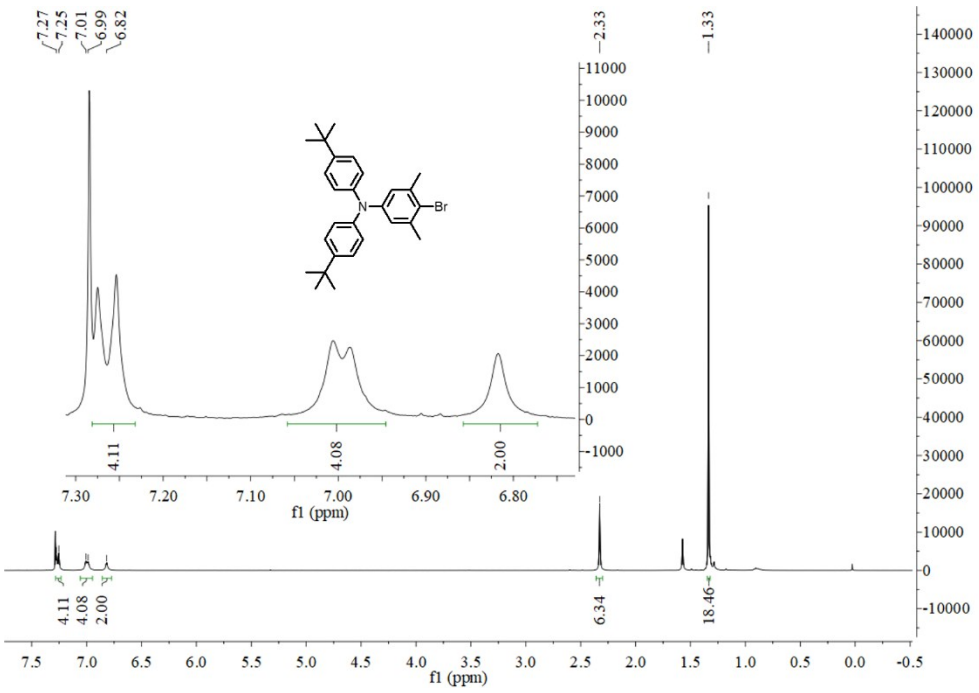

Figure S13. ^{1}H NMR spectrum of **DMeTPA-Br**

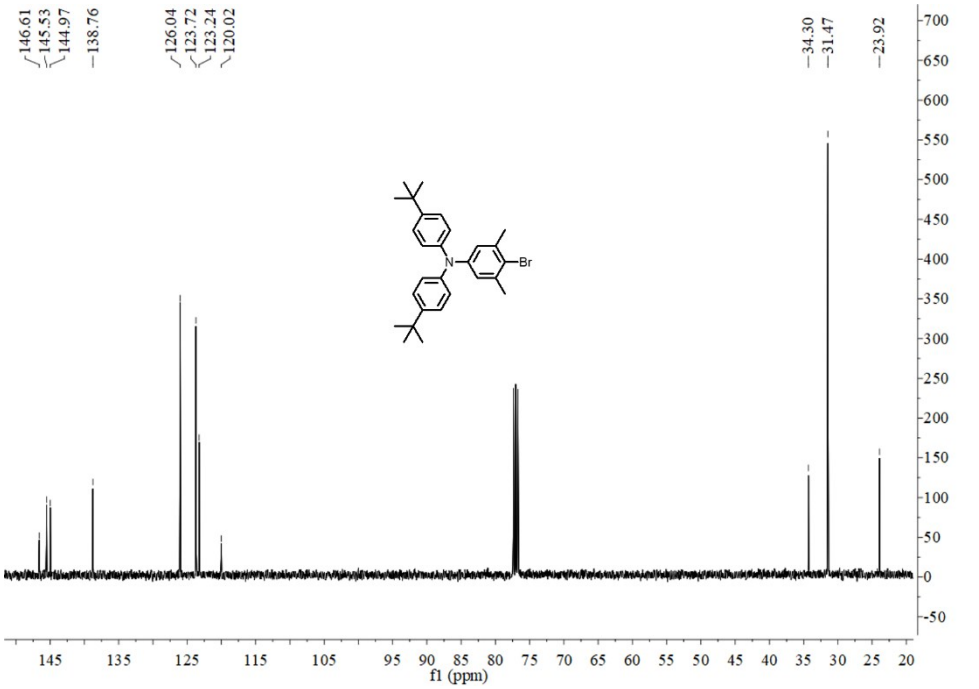

Figure S14. ^{13}C NMR spectrum of **DMeTPA-Br**

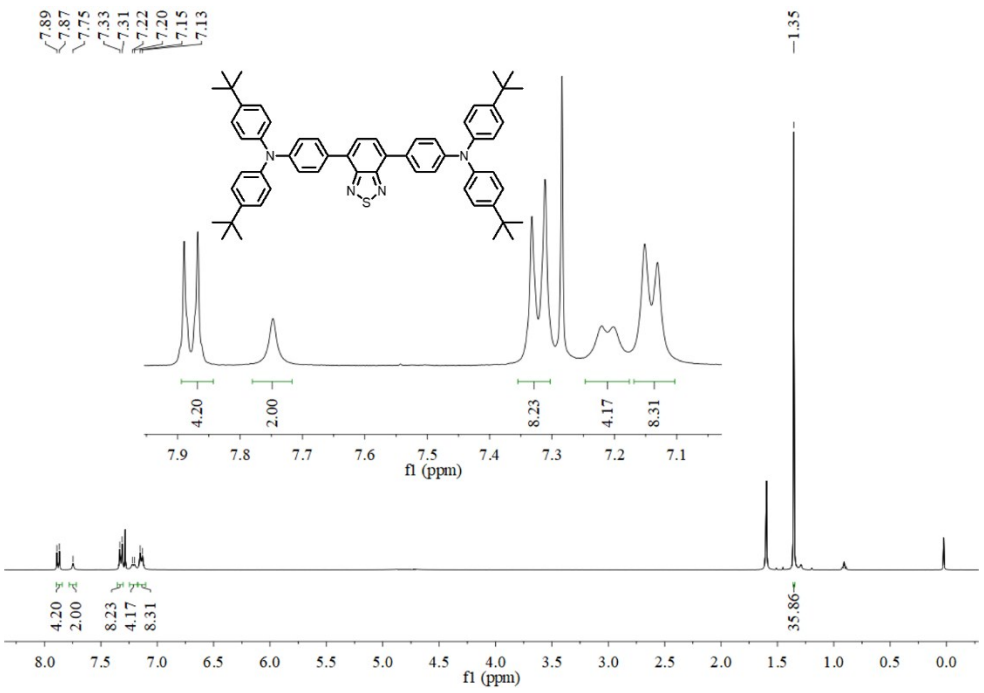

Figure S15. ^{1}H NMR spectrum of **2TPA-BT**

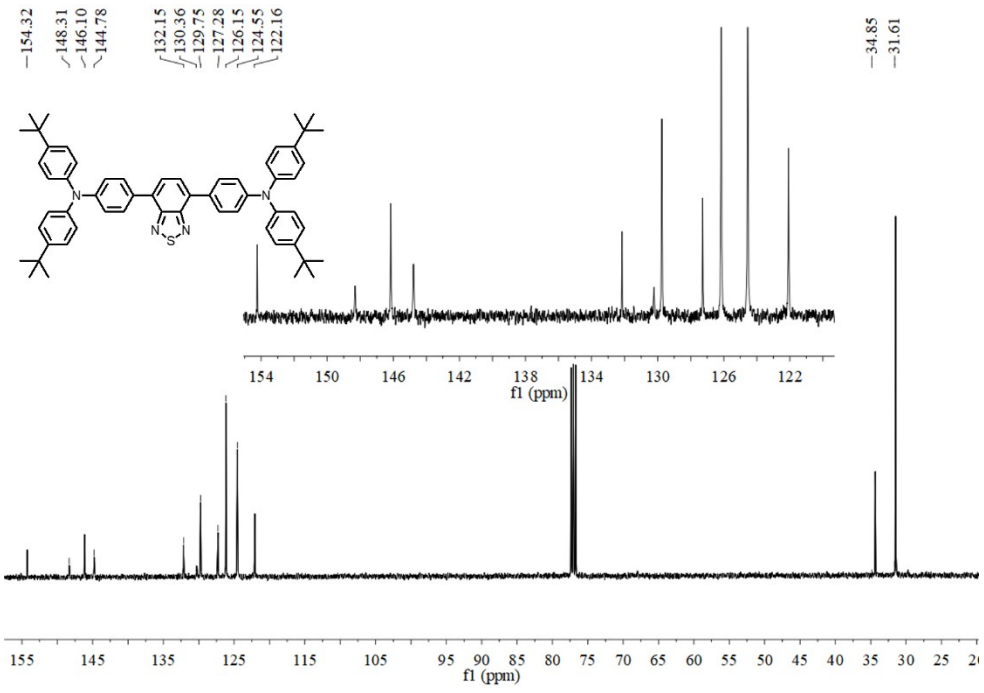

Figure S16. ^{13}C NMR spectrum of **2TPA-BT**

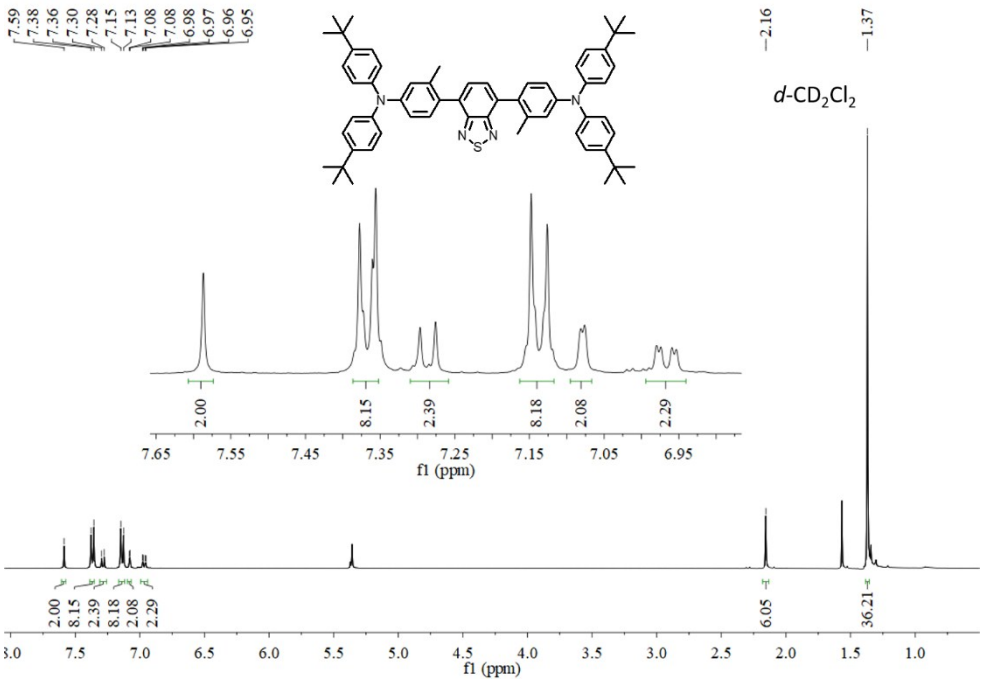

Figure S17. ^{1}H NMR spectrum of **2MeTPA-BT**

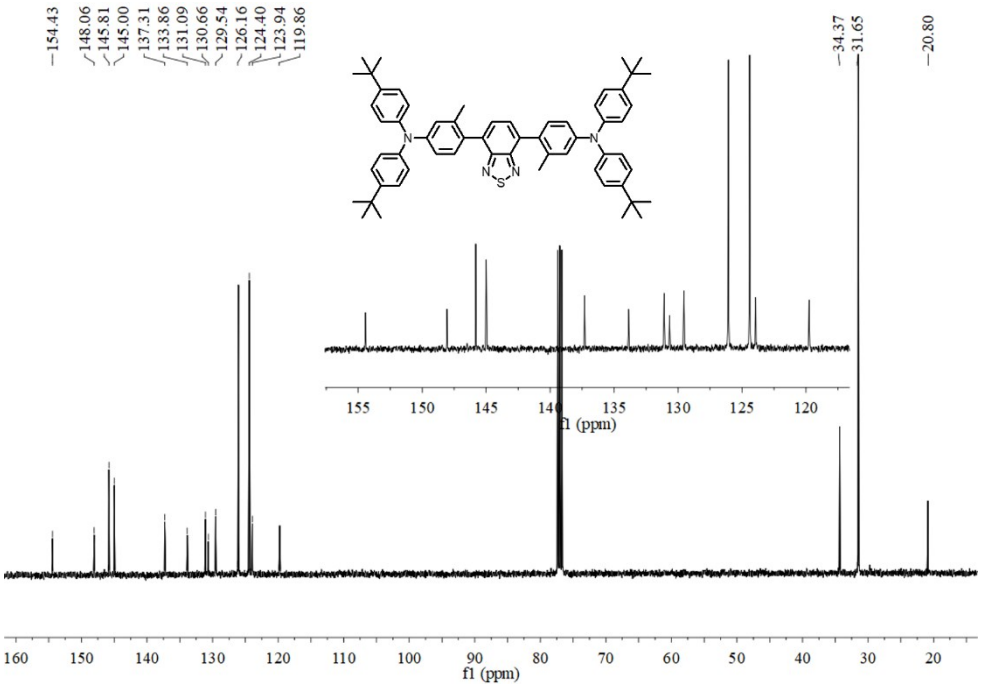

Figure S18. ^{13}C NMR spectrum of **2MeTPA-BT**

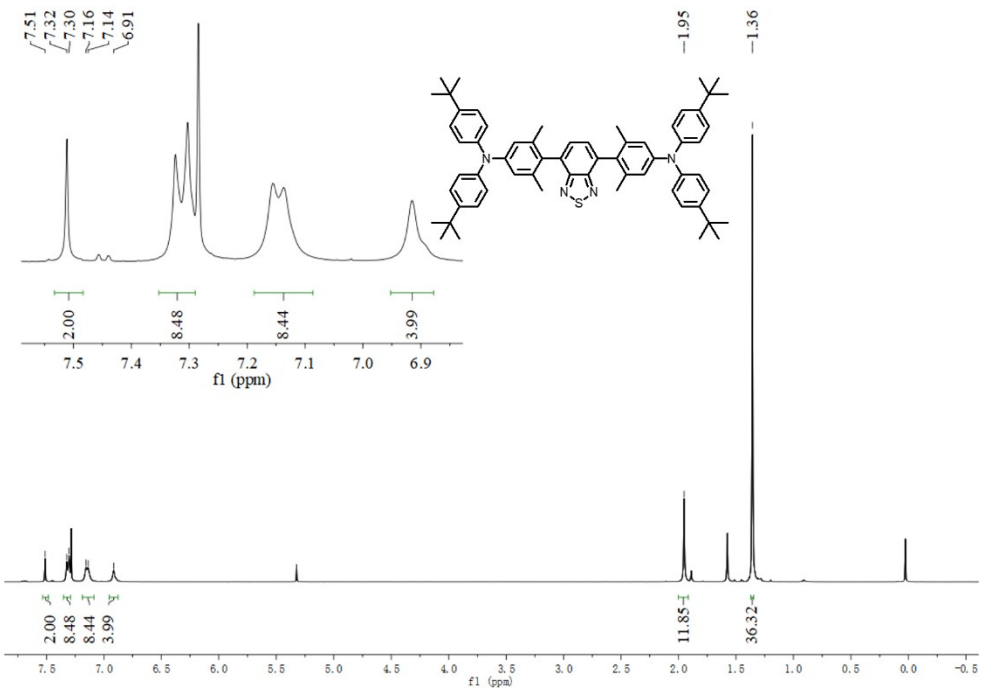

Figure S19. ^{1}H NMR spectrum of **2DMeTPA-BT**

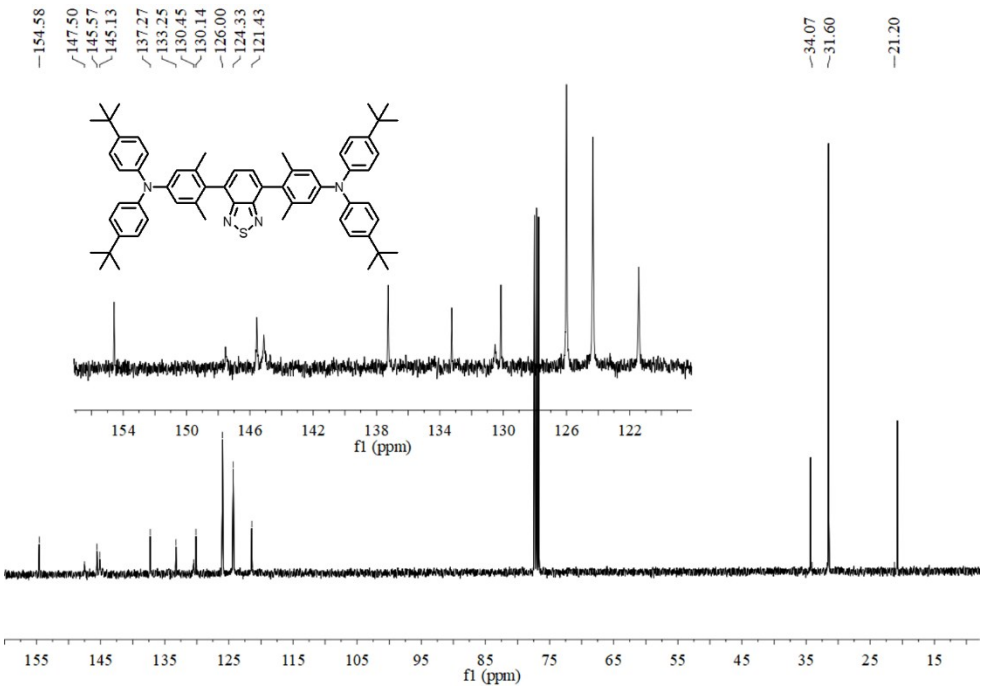

Figure S20. ^{13}C NMR spectrum of **2DMeTPA-BT**

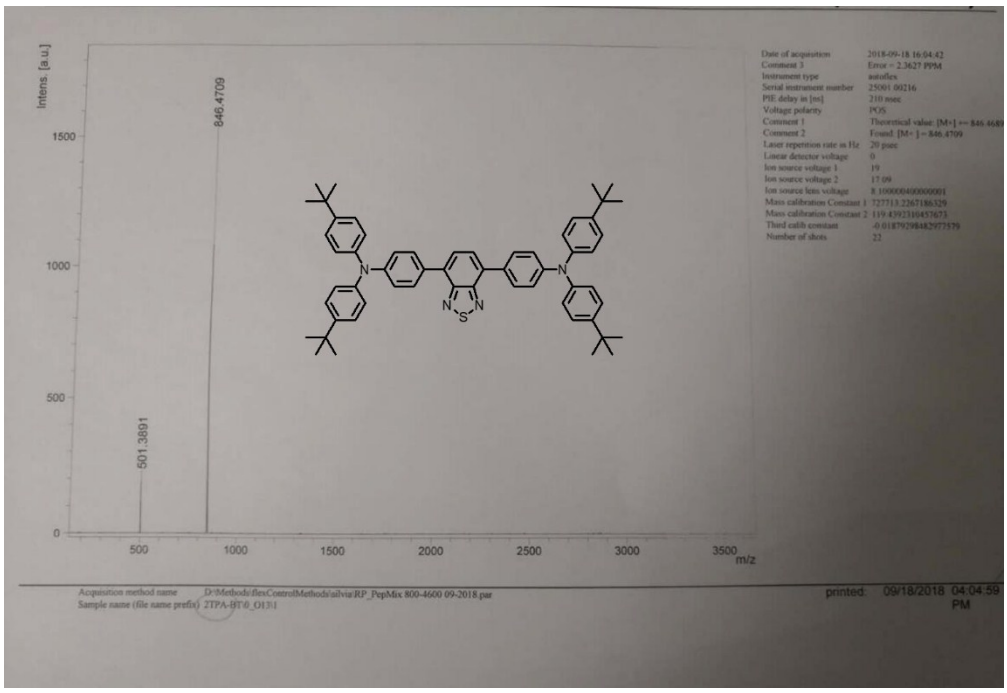

Figure S21. MALDI-TOF mass spectrum of **2TPA-BT**

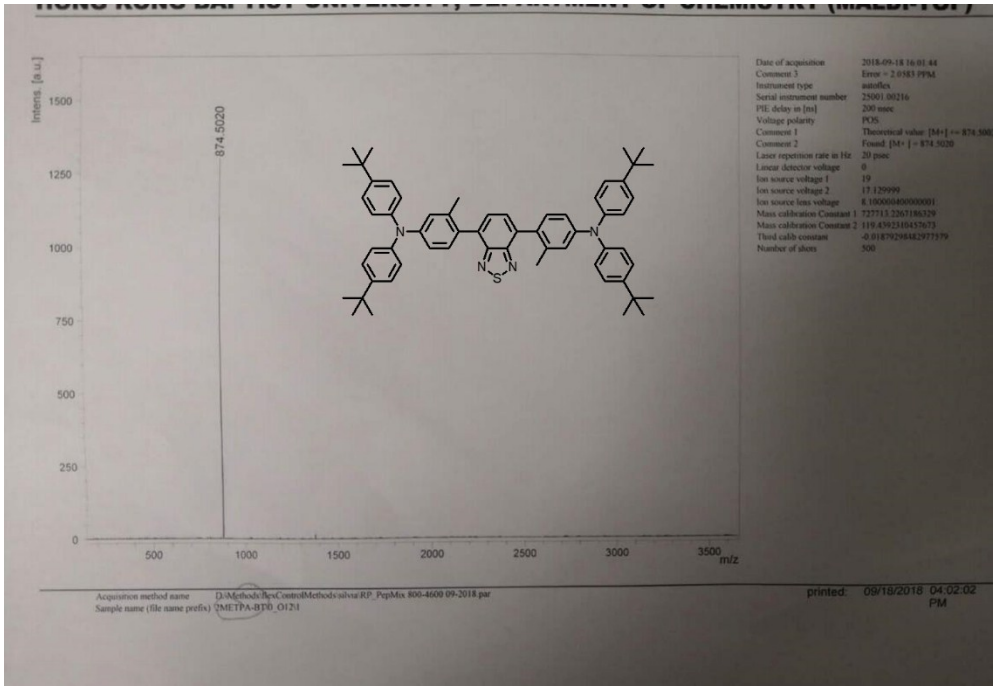

Figure S22. MALDI-TOF mass spectrum of **2MeTPA-BT**

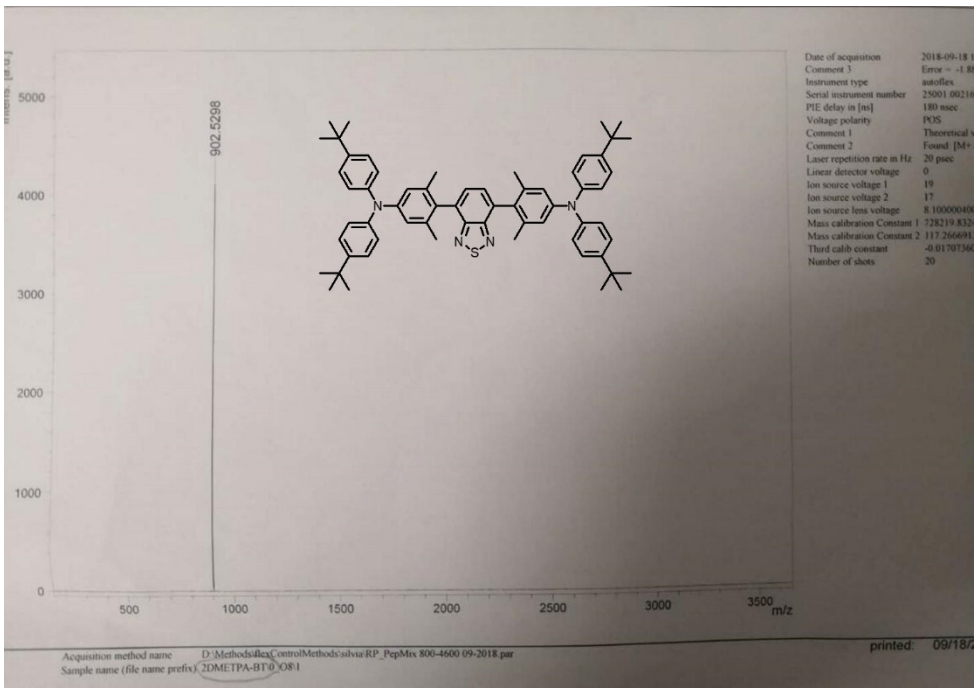

Figure S23. MALDI-TOF mass spectrum of **2DMeTPA-BT**